Biochimica et Biophysica Acta 1848 (2015) 167–173

Contents lists available at ScienceDirect

Biochimica et Biophysica Acta

journal homepage: www.elsevier.com/locate/bbamem

Phospholipid lateral diffusion in phosphatidylcholine-sphingomyelin-cholesterol monolayers; Effects of oxidatively truncated phosphatidylcholines

Petteri Parkkila [a,1], Martin Štefl [b,1,2], Agnieszka Olżyńska [b], Martin Hof [b], Paavo K.J. Kinnunen [a,*]

[a] Helsinki Biophysics & Biomembrane Group, Department of Biomedical Engineering and Computational Science, School of Science, Aalto University, Espoo, Finland
[b] J. Heyrovský Institute of Physical Chemistry of the Academy of Sciences of the Czech Republic, v. v. i., Dolejškova 2155/3, 182 23 Prague 8, Czech Republic

ARTICLE INFO

Article history:
Received 2 July 2014
Received in revised form 10 October 2014
Accepted 20 October 2014
Available online 25 October 2014

Keywords:
Oxidatively truncated phosphatidylcholines
Lateral diffusion
Fluorescence correlation spectroscopy
Langmuir monolayers
Liquid ordered phase

ABSTRACT

Oxidative stress is involved in a number of pathological conditions and the generated oxidatively modified lipids influence membrane properties and functions, including lipid–protein interactions and cellular signaling. Brewster angle microscopy demonstrated oxidatively truncated phosphatidylcholines to promote phase separation in monolayers of 1-palmitoyl-2-oleoyl-*sn*-glycerol-3-phosphocholine (POPC), sphingomyelin (SM) and cholesterol (Chol). More specifically, 1-palmitoyl-2-azelaoyl-*sn*-glycero-3-phosphocholine (PazePC), was found to increase the miscibility transition pressure of the SM/Chol-phase. Lateral diffusion of lipids is influenced by a variety of membrane properties, thus making it a sensitive parameter to observe the coexistence of different lipid phases, for instance. The dependence on lipid lateral packing of the lateral diffusion of fluorophore-containing phospholipid analogs was investigated in Langmuir monolayers composed of POPC, SM, and Chol and additionally containing oxidatively truncated phosphatidylcholines, using fluorescence correlation spectroscopy (FCS). To our knowledge, these are the first FCS results on miscibility transition in ternary lipid monolayers, confirming previous results obtained using Brewster angle microscopy on such lipid monolayers. Wide-field fluorescence microscopy was additionally employed to verify the transition, i.e. the loss and reformation of SM/Chol domains.

1. Introduction

Lipid oxidation has profound effects on the biophysical properties of lipid membranes, and alterations such as phase changes and phase separation in model membranes have been demonstrated. Interest in the effects of oxidized lipids on membrane biophysics was revived upon the availability of well-defined, stable oxidatively modified phospholipid derivatives together with recent advances in cell biology pointing to the involvement of oxidized lipids in processes such as inflammation and apoptosis and the molecular pathology of several neurodegenerative diseases [1,2]. Along these lines it was shown that the addition of oxidatively truncated phosphatidylcholines into fluid phase 1-palmitoyl-2-oleoyl-*sn*-glycerol-3-phosphocholine (POPC) bilayers caused a loss of the permeability barrier function of the lipid bilayers, together with rapid loss of lipid asymmetry [3]. The latter finding is of significance as it undermines the notion of a specific transmembrane protein (flippase/scramblase) being responsible for the transfer of phosphatidylserine from the inner to the external leaflet of the plasma membrane lipid bilayer in apoptosis [4,5].This was substantiated in computer simulations, highlighting the importance of detailed understanding of lipid biophysics deciphering potential new physiologically meaningful functional consequences of changes in lipid composition, thus introducing a new paradigm to the analysis of cell behavior, which at present is almost exclusively being explained in terms of activities of specific proteins, enzymes, receptors, channels, and so on.

Along somewhat similar lines it was shown that the introduction of an oxidatively truncated phosphatidylcholine derivative PazePC promotes in lipid monolayers the phase separation of a lipid phase consisting of sphingomyelin and cholesterol. The aim of the present study was quantitative analysis of the diffusional dynamics of membranes containing the oxidatively truncated phosphatidylcholines (PazePC and PoxnoPC, Fig. 1) included into monomolecular films of sphingomyelin, cholesterol, and POPC. We could confirm that the

Abbreviations: AOM, acousto-optical modulator; AOTF, acousto-optical tunable filter; BSA, bovine serum albumin; Chol, cholesterol; FCS, fluorescence correlation spectroscopy; FRAP, fluorescence recovery after photobleaching; L_d, liquid disordered phase; L_o, liquid ordered phase; NMR, nuclear magnetic resonance; oxPC, oxidatively modified phosphatidylcholines; oxPL, oxidized phospholipids; PazePC, 1-palmitoyl-2-azelaoyl-*sn*-glycero-3-phosphocholine; POPC, 1-palmitoyl-2-oleoyl-*sn* glycerol-3-phosphocholine; POPE, 1-palmitoyl-2-oleoyl-*sn*-glycero-3-phosphoethanolamine; PoxnoPC, 1-palmitoyl-2-(9′-oxononanoyl)-*sn*-glycero-3-phosphocholine; SM, sphingomyelin; SPT, single particle tracking; WFM, wide-field fluorescence microscopy

* Corresponding author at: Helsinki Biophysics & Biomembrane Group, Department of Biomedical Engineering and Computational Science, P.O. Box 12200 (Rakentajanaukio 3), FIN-00076 Aalto, Finland. Tel.: +358 505404600; fax: +358 947023182.
E-mail address: paavo.kinnunen@aalto.fi (P.K.J. Kinnunen).
[1] These authors contributed equally to this work.
[2] Present address: Zentrum für Molekulare Biologie der Universität Heidelberg, Im Neuenheimer Feld 282, 691 20 Heidelberg, Germany.

http://dx.doi.org/10.1016/j.bbamem.2014.10.025
0005-2736/

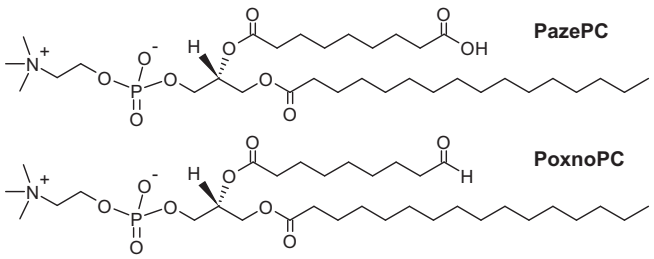

Fig. 1. Chemical structures of two oxidatively truncated phosphatidylcholines, PazePC and PoxnoPC.

miscibility transition pressure, the melting pressure of liquid-ordered (l_o) SM/Chol-domains, tends to increase with increasing the content of oxidized phospholipids (oxPLs) [6]. The results were interpreted in terms of line tension outweighing dipolar interactions in maintaining domain structure and shape due to the lack of differences in the average dipole density upon the mixing of the phases [7,8]. Most importantly, PCs with oxidatively truncated acyl chains increase the thickness mismatch between the coexisting phases, contributing to the line tension at the domain boundaries. This is further associated with the complete chain-reversal of the truncated acyl chains [9]. We aimed at investigating if the above also involves changes in lateral lipid mobility. Lateral self-diffusion is sensitive to a number of diverse changes in lipid bilayer properties and may give more insight into lipid film behavior during the compression and domain disintegration. To answer the question in which way is the vicinity of domains and oxPL affecting the lateral self-diffusion, we compared SM/Chol-enriched films with monolayers containing phospholipids only, while varying the content of oxPL in the phosphatidylcholine fraction.

For this utility, we assembled a fluorescence correlation spectroscopy (FCS) z-scan setup for continuous scanning of the fluorescence correlation time traces during compression of lipid monolayers. A similar system has previously been described by Gudmand et al. [10]. Several methods are available to measure membrane diffusional dynamics, the most popular being fluorescence recovery after photobleaching (FRAP), single particle tracking (SPT), and pulsed field gradient NMR [11–13]. Apart from the latter, these are all light microscopy methods. While FRAP measurements are affected by monolayer surface flow, and SPT can be experimentally demanding, FCS provides with the properties well applicable for monolayer experiments. Light microscopy diffusion methods are discussed in detail by Chen et al. [14].

2. Theory

In general, lateral self-diffusion due to the thermal collisions can be characterized by:

$$(r(t)-r(0))^2 = 4Dt^{\alpha}, \tag{1}$$

which describes the time dependence of the mean square displacement of a particle over long time scales. The diffusion coefficient D and anomalous factor α are sufficient to describe the diffusion of the particle. The parameter α can be assumed to be one for homogenous distribution of the self-diffusing molecules and <1 for hindered diffusion.

2.1. FCS

FCS is very well suited for use with Langmuir films, making it possible to observe anomalous dynamic components from the auto-correlation curves and still maintain statistical single-molecule sensitivity. The downside of this approach is the depth of the observation volume (~1–2 μm) in comparison with the monolayer thickness (nm), which makes it difficult to have the monolayer coincide with the scanner position. Likewise, while contact of the film with water corresponds to real molecular interactions of biomembranes, surface evaporation could be a challenge. As stated in previous studies, fluorescence correlation spectroscopy (FCS) is a powerful statistical method in analyzing lateral diffusion in membranes [15]. A confocal microscopy setup is utilized to focus laser light through an objective with high numerical aperture into a small detection volume (V ~ 1 fl), while the fluorescence light emitted from molecules diffusing through the detection volume is collected and analyzed. The number of fluorescent species has to be low enough in order to have substantial signal contribution from each diffusing molecule (usually in nanomolar range). For analysis, auto-correlation function is calculated for the detected signal.

For a two-dimensional sample, assumption of Gaussian detection profile yields:

$$G(\tau) = 1 + \frac{1}{N}\left(\frac{1}{1+\frac{\tau}{\tau_D}}\right), \tag{2}$$

where the fluctuating signal is analyzed with respect to its self-similarity after the lag time τ. N is the mean number of fluorophores in the focus, and τ_D is the average time for a single fluorescent molecule to diffuse through the detection area. The minimum of both these parameters is found in the exact beam waist of the confocal volume.

When other photophysical events (e.g. intersystem crossing) are contributing to the overall fluorescence signal, an average fraction of fluorophores in triplet state T and intersystem crossing relaxation time τ_T need to be implemented into Eq. (2) [16] and the autocorrelation function thus becomes:

$$G(\tau) = 1 + \left[1-T+Texp\left(\frac{-\tau}{\tau_T}\right)\right]\frac{1}{N(1-T)}\frac{1}{1+\left(\frac{\tau}{\tau_D}\right)}. \tag{3}$$

Moreover, in the case of two fluorescent species laterally diffusing through the detection volume, Eq. (3) has to be expanded:

$$G(\tau) = 1 + \left[1-T+Texp\left(\frac{-\tau}{\tau_T}\right)\right]\frac{1}{N(1-T)}\left(\frac{Amp}{1+\left(\frac{\tau}{\tau_{Da}}\right)}+\frac{1-Amp}{1+\left(\frac{\tau}{\tau_{Db}}\right)}\right), \tag{4}$$

where τ_{Da} and τ_{Db} correspond to the diffusion times of two fluorescent species with different diffusing properties and Amp is the amplitude of auto-correlation corresponding to faster diffusing species τ_{Da}. One can further relate the diffusion coefficient with the diffusion time by:

$$D = \frac{\omega^2}{4\tau_D}, \tag{5}$$

where ω is the radius of the cross-sectional area of the detection volume. Due to the variation in the axial positioning of the sample relative to the scanner, we could not determine the exact values of ω. Therefore we are limited to interpret individual diffusion times as a relative measure of the diffusional lipid dynamics. Large amount of auto-correlation functions in relation to the surface pressure, and area, were obtained and could be satisfactorily fitted by Eqs. (3) and (4), respectively.

2.2. Free-area model

Free-area model for self-diffusing particles has been known for decades and has proven to be useful in single-lipid studies [17–19]. Due to the discrepancies with the experiments involving multiple lipid species, we do not intend to use it for our ternary "raft mixture" studies [20,21]. Free-area model relates diffusion to the available free area in a lateral lipid lattice, $a_f = a - a_0$, where a is the molecular area obtained from Langmuir experiments, and a_0 is the core area of a single lipid

(~ 42 Å^2 for a phospholipid). The model is described by the following equation:

$$\ln \frac{D}{D_{max}} = -\gamma \frac{a_c}{a_f}, \quad (6)$$

where D_{max} represents the maximal diffusion coefficient corresponding to a gaseous monolayer, a_c is the critical area per molecule where lateral diffusion becomes possible, and γ is a constant describing the overlapping of free areas ($0.5 < \gamma < 1$). Given the inverse proportionality between D and τ_D (when ω is constant), we can approximate:

$$\ln \frac{\tau_D}{\tau_{min}} = \gamma \frac{a_f}{a_c} = \frac{\beta}{a_f}, \quad (7)$$

where τ_{min} is the fastest diffusion time of the fluorescent probe in a monolayer.

3. Materials and methods

3.1. Materials

Bovine serum albumin (BSA) and NaCl were from Sigma (St. Louis, MO). 1-palmitoyl-2-azelaoyl-*sn*-glycero-3-phosphocholine (PazePC), 1-palmitoyl-2-oleyl-*sn*-glycero-3-phosphocholine (POPC), 1-palmitoyl-2-(9′-oxononanoyl)-*sn*-glycero-3-phosphocholine (PoxnoPC), 1-palmitoyl-2-oleoyl-*sn*-glycero-3-phosphoethanolamine (POPE), cholesterol (Chol), and porcine brain sphingomyelin (SM) were purchased from Avanti Polar Lipids (Alabaster, AL). Atto-488-NSH-ester (Atto-TEC, Siegen, Germany) was covalently reacted with POPE, followed by separation of the free, non-reacted dye from the labeled lipid (POPE-Atto488) using chromatography on a silica gel column. Dye to lipid molar ratios of 1:300 000 and 1:1000 were used in FCS and wide-field microscopy measurements, respectively.

3.2. Methods

3.2.1. Langmuir films

A commercial Langmuir trough (μtrough XS; Kibron, Helsinki, Finland) was used to measure surface pressure ($\Pi = \gamma - \gamma_0$, where γ_0 stands for surface tension of pure subphase) as a function of mean molecular area *a*. Physical trough area was controlled with two symmetrically moving Teflon-barriers by using dedicated software provided by the equipment manufacturer, while surface tension/pressure was detected by a Ni-chrome wire attached to a microbalance [22]. Notably, unlike for the conventionally employed Pt probes, the receding and advancing contact angles for Ni-chrome are identical and thus avoid artefactual hysteresis between film compression and relaxation (Momsen et al. [22]). Lipids in chloroform were spread onto air–water interface with a Hamilton syringe. Aqueous 150 mM NaCl was used as a subphase.

Because of the very short (0.28 mm) working distance of the objective, a rubber spacer was inserted to elevate the cover glass window in the bottom of the Langmuir trough. The cover glass was saturated with bovine serum albumin in order to decrease the hydrophobicity of the glass coverslip. Water evaporation turned out to be an issue, and was avoided by pumping buffer in the trough behind the moving teflon barrier. The rate of buffer addition adjusted to compensate for the evaporation during the measurement. In addition, to reduce the surface flow and to maintain constant experimental conditions, a transparent partially-sealed box was used to enclose the trough. A constant temperature of T = 24 °C was maintained during all FCS and WFM measurements.

3.2.2. FCS experimental setup

The FCS measurements were performed on a home-built inverted confocal microscope setup based on Olympus IX 71 (Olympus, Hamburg, Germany) microscope body. The dye was excited by Picosecond Laser Diode (LDH-P-C-470B, PicoQuant GmbH, Germany) and the excitation laser intensity was controlled by acousto-optical modulator AOM (MT200A0.5-VIS, AA OPTO-ELECTRONIC, Orsay, France). Collimated excitation laser beam was reflected by appropriate dichroic mirror (Chroma Technology Corporation, VT, USA) and was focused by water immersion objective (Olympus, 60×, NA 1.2, WD 0.28 mm) into the sample. Emitted fluorescence light was subsequently collected by the same objective and after passing through an emission filter (515/50, Omega Optical, VT, USA), it was detected on SPAD detector (MPD, PicoQuant GmbH, Berlin, Germany). The fluorescence coming from out-of-focus axial planes was cut using a 50 μm pinhole. The laser intensity was kept under 10 μW to prevent photobleaching and detector saturation.

3.2.3. Z-scan measurements

In order to reach correct diffusion times, where the monolayer is exactly in the beam waist minimum of the detection volume, positional scanning along the optical axis was performed (z-scan) [23]. During the compression process, multiple z-scans were performed while continuously measuring surface pressure. Each z-scan consisted of several FCS traces (10 s each) which were recorded in step-wise manner. Subphase position was checked and adjusted between each scan. The axial positioning during z-scan FCS was supplied by piezo system (PI P-562, Karlsruhe, Germany) and the step between individual measurements was 200 nm. The fluorescence intensity fluctuations were correlated and further analyzed using Origin software (OriginLab Corporation, MA, USA) by assuming Gaussian cross section of the focus (Eqs. (3) and (4)).

3.2.4. WFM

The imaging experiments were performed on a home-built inverted wide-field microscope (WFM) which consisted of the same microscope body as used for FCS. We used continuous excitation (Coherent, Saphire 488-150CW, CA, USA) modulated by acousto-optical tunable filter (AOTFnC-400.650-TN, AA OPTO-ELECTRONIC, Orsay, France). The sample was illuminated by water immersion objective (Olympus, 60×, NA 1.2, WD 0.28 mm) and the same objective was used for the collection of emitted light. The emitted photons passed through the emission filter (515/50, Omega Optical, VT, USA) and were detected by a CCD camera (Andor, Belfast, UK). The pixel size was 167 nm, frame rate 1/30 ms. The laser intensity was varied during the experiments to get best imaging contrast and to prevent the saturation of camera. The images were processed using ImageJ and Origin softwares.

4. Results

4.1. Oxidized phospholipids in POPC monolayers

In order to understand the influence of the oxidatively truncated PCs on the diffusional dynamics in lipid monolayers, FCS measurements were performed while the monolayers were compressed and surface pressure was measured. First, to test the approach and to better understand the behavior of the system, a binary mixture of POPC and PazePC with an oxidatively truncated acyl chain with a terminal carboxylic acid moiety in *sn*-2 position of the backbone glycerol was used. A comparison of POPC films with those additionally containing 25 mol% of PazePC did not reveal any obvious changes in the slope of the linear dependence of diffusion time (one component model, Eq. (3)) versus surface pressure (Fig. 2A). These findings are in agreement with *in vitro* measurements on lateral diffusion lipid bilayers, where addition of similar oxidatively modified phospholipid PGPC (where truncated acyl chain is about 4 carbon atoms shorter in comparison to PazePC) did not result in significant changes in lateral diffusion [24,25]. Instead, the differences

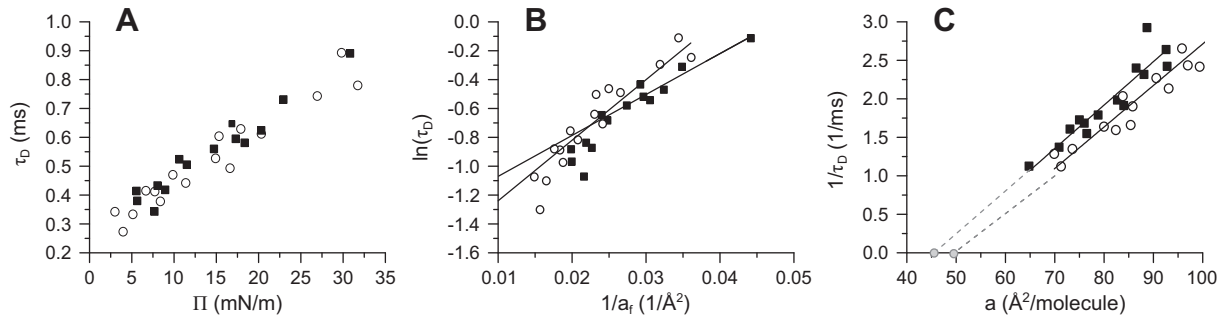

Fig. 2. Diffusion time measurements for POPC/PazePC films at 25 °C with 0% (■) and 25% (○) of PazePC. (A) Diffusion time τ_D vs. surface pressure Π. (B) ln τ_D vs. inverse of free area a_f. (C) Inverse of τ_D vs. molecular area a.

become evident when the logarithm of τ_D is plotted against the reciprocal value of free area a_f (Fig. 2B), which is in accordance with the free-area model. The kink at $a_f^{-1} \approx 0.022$ Å^{-2} suggests that the model seems to fail for dilute films ($a > 87$ Å^2), as observed previously [9]. When the linear fits of molecular area versus $1/\tau_D$ (Fig. 2C) are extrapolated to infinitely long diffusion times (i.e. no diffusion), the critical areas for those compositions can be estimated. We have determined the values of ~ 46 Å^2 and ~ 50 Å^2 for pure POPC and POPC/PazePC mixture, indicating slight area expansion for the latter film. Values for different parameters are summarized in Table 1. Higher β-values indicate that when the free area decreases, the diffusion time will increase more rapidly in POPC/PazePC. Overlapping-factor γ was estimated by dividing the value of β obtained from the free-area model (Fig. 2B) by the extrapolated critical molecular area a_c (Fig. 2C). Yet, this is a rough estimate and should be considered as tentative value only.

Since relatively large hysteresis was detected in all pressure-area isotherms during compression–expansion cycles (data not shown), stable constant-area measurements of surface pressure could not be obtained. The rapid nature of the drop in surface pressure indicates that the observed hysteresis was not caused by oxidation of POPC which has been shown to be more resistant to oxidation-induced surface pressure drop than other unsaturated phospholipids [26–28]. The fast drop could indicate both film relaxation due to the abruptly stopped compression and high sensitivity of the metal probe. The latter was also observed during the sensor calibration. However, no significant area loss or reduction in fluorescence signal was detected during the first two compression-expansion cycles.

4.2. Oxidized phospholipids in a ternary "raft mixture"

Lipid monolayers with coexisting liquid ordered/condensed and disordered/expanded phases were examined for the influence of oxidized phospholipids. POPC/SM/Chol mixtures in the molar ratio of 1.5/1.5/1 were chosen in order to mimic lipid compositions in mammalian cell membranes and also for the possibility to follow micrometer-size lipid domains by optical microscopy. For samples containing oxidatively truncated PCs, 12.5 or 25% of POPC fraction (i.e. 4.7 or 9.4 mol% of the overall lipid mixture) was substituted by PazePC or PoxnoPC, respectively. The monolayer was stained with POPE-Atto488 and we did not find any significant partitioning of the fluorophores into the liquid ordered phase in neither confocal nor wide-field microscopy.

Table 1
Free-area model parameters obtained from Fig. 2B. Value of γ is estimated by dividing the value of β with extrapolated critical area from Fig. 2C.

	POPC	POPC/PazePC (75:25)
β	28 ± 2.9	42 ± 5.8
τ_{min} (ms)	0.19 ± 0.05	0.17 ± 0.06
a_c (Å^2)	46	50
γ	0.61	0.84

WFM imaging provided information on the morphology of the L_o-domain structures upon compression and subsequent expansion (Fig. 3). The experiments were performed for a lipid mixture with no oxPL and for mixtures with 9.4 mol% of PazePC or PoxnoPC, as indicated. During early stages of monolayer compression, domains preserve their distinct circular shape until the onset of the miscibility transition (at 12 mN/m for the film without oxPLs, 15 mN/m and 18 mN/m for films with 9.4 mol% PazePC or PoxnoPC, respectively). Thus, the domains remain unaffected by the compression, reducing the free area for phospholipid molecules to diffuse in the L_d-phase. Higher miscibility transition pressure values for oxPL-containing lipid films confirm stabilization of phase separation in lipid monolayers by oxPLs, as shown previously [6]. We did not measure diffusion in the L_o-phase; however the integrity of domain structures was seen in all films.

The size of the domains is slightly smaller for the oxPL-containing films (domain size distributions are (2.12 ± 0.61) μm, (1.91 ± 0.39) μm and (2.05 ± 0.48) μm for oxPL-free, PazePC and PoxnoPC monolayers, respectively (Fig. 4)), which could indicate oxidation-induced increase in line tension, the main factor contributing to the domain stability [8]. When miscibility transition pressure is crossed, the domains lose their integrity and fluorescently labeled lipid can enter them, evident as loss of domain structure. The reformation of domains during the monolayer expansion could indicate relative system stability for lipid films free of oxPLs and those with PazePC. Surprisingly, expansion of PoxnoPC containing samples results in highly inhomogeneous system in terms of domain morphology. While there were no differences in miscibility transition pressures for compression and expansion in PazePC films, a slight transition pressure drop was detected in films with no oxPL and also with PoxnoPC. In addition, few circular domains can be still seen in POPC/SM/Chol films after the transition. It would seem that there is some fluorophore partitioning into these domains, resulting in a lower image contrast.

FCS measurements were performed during film compression in order to quantify the impact of oxPLs on the domain structures in the monolayers. In most of the intensity time traces a surface flow of the whole system was observed, which results in sudden decrement in fluorescence signal because of the presence of non-fluorescent structures in the detection volume. Despite such inhomogenous fluorophore distribution, the time scales of the domains wandering through the focus due to the surface flow were found to be a three orders of magnitude slower (1–2 s) than the lateral diffusion of fluorescent lipid in the monolayer (~ ms). This made it possible to analyse intensity time traces using autocorrelation analysis (two component model, for details see Eq. (4)) in spite of the sudden decrement in the fluorescence signal.

We did a continuous compression while obtaining FCS data, which revealed distinct sigmoidal diffusion behavior as the surface pressure increases (Fig. 5A). The upper and lower limits in diffusion time can be found from the Boltzmann fits of the data. Diffusion times reach maximum value of τ_D ~ 1.5 ms for samples with and without oxPLs. Similarly, the minimal diffusion time of 0.29 ms was found in low surface pressures regardless of the L_d-phase composition. As expected, zero

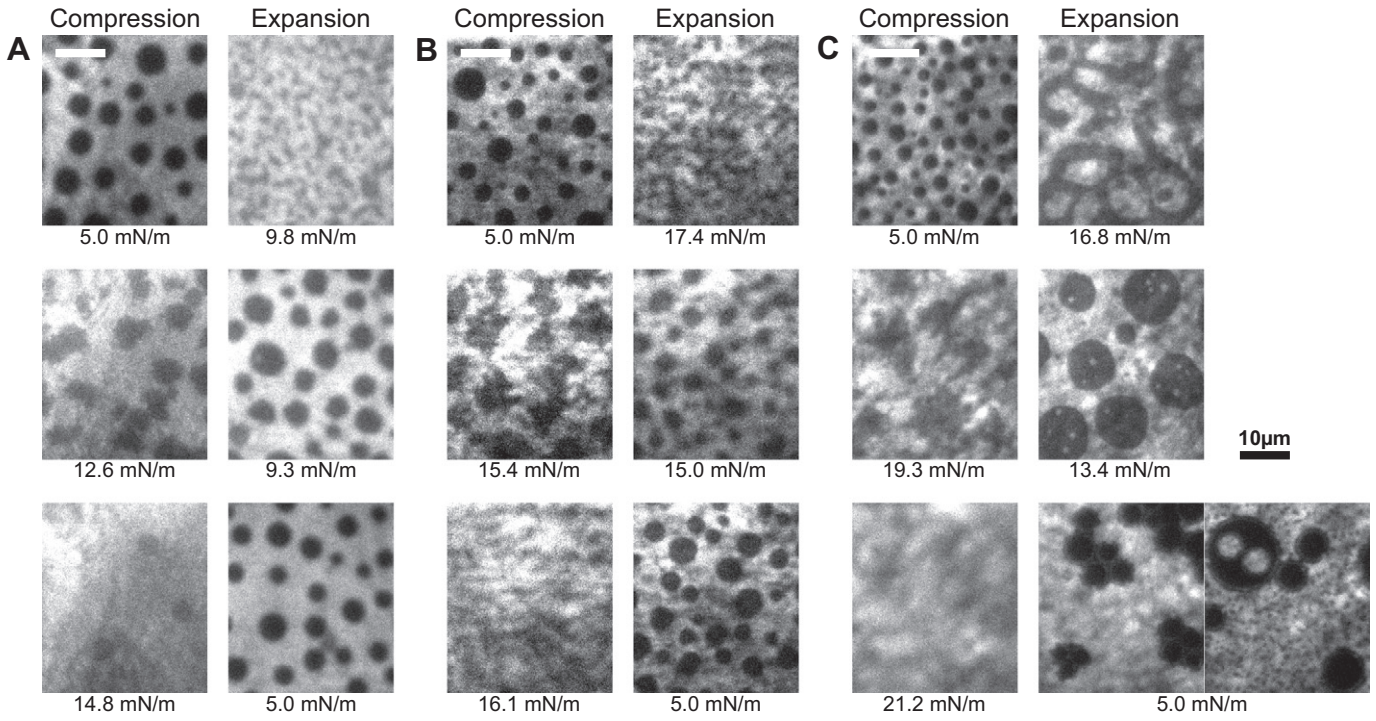

Fig. 3. WFM imaging of monolayer compression and expansion cycles at 24 °C. Panel A) corresponds to POPC/SM/Chol (1.5/1.5/1 molar ratio), while panels B) and C) show monolayers where 25% of POPC is substituted by 9.4 mol% PazePC (panel B) or 9.4 mol% PoxnoPC (panel C). Note that completely expanded monolayer in lipid samples containing PoxnoPC is highly heterogeneous.

values of the second derivatives of the corresponding Boltzmann fits (i.e. the pressures yielding maximal diffusion slowdown) are close to the miscibility transition pressures found in wide field microscopy (Fig. 5B). Boltzmann fits give the value of 11.7 mN/m for films without oxPLs (12 mN/m in WFM) and 18.7 mN/m and 20.4 mN/m for 9.4 mol% PazePC (15 mN/m in WFM) and PoxnoPC (18 mN/m in WFM), respectively. Thus, a quantitative prediction of miscibility transition pressures can be obtained from the diffusion time measurements. For both systems containing oxPLs the quantitative values determined by FCS are slightly higher than those observed in WFM. However, in the case of WFM, the determination of phase transition pressure relies on subjective visual observation. Also, the non-equilibrium state (until

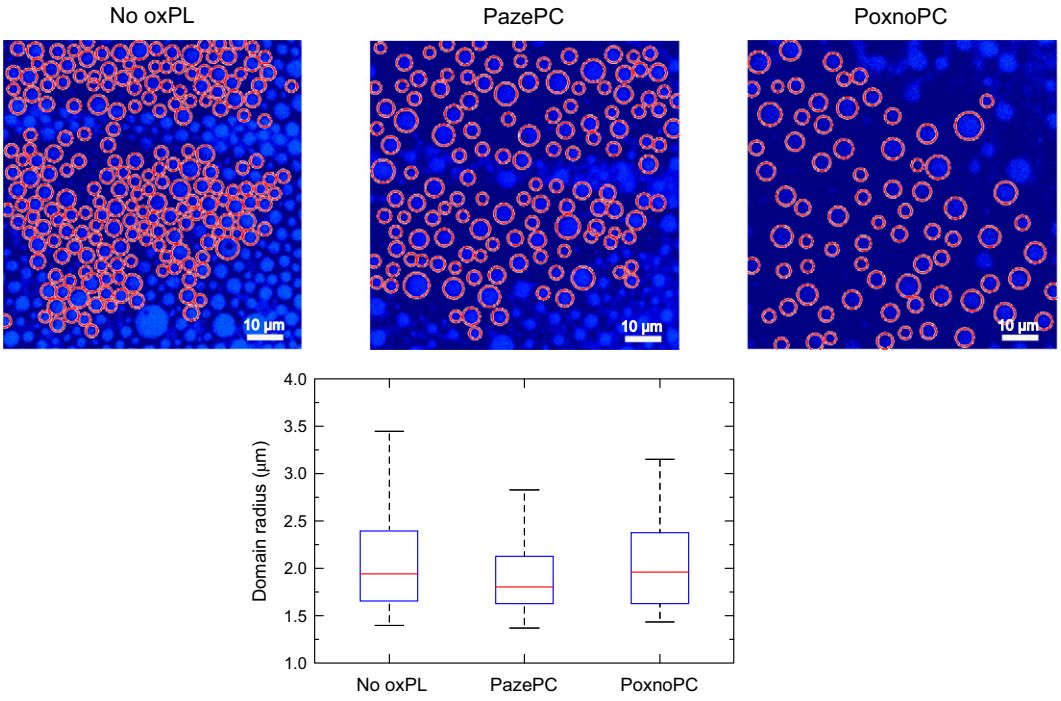

Fig. 4. Upper part: Segmented images of various systems before the compression started. Only those structures with high contrast have been segmented. The number of analyzed structures is as follows; $n = 376$ for system without oxPLs, $n = 208$ and $n = 109$ for monolayers containing PazePC and PoxnoPC, respectively. Lower part: Statistical data from segmentation. Red line corresponds to the median of segmented domain radii. First and third quartile is depicted as blue box and dashed lines show the interval of analyzed domain radii.

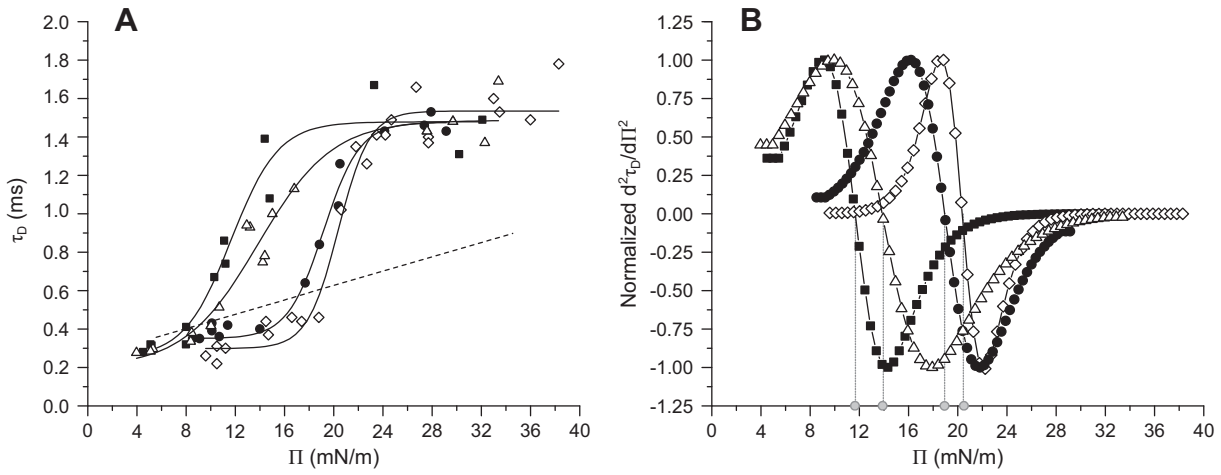

Fig. 5. (A) Diffusion time τ_D vs. surface pressure Π and (B) second derivative of τ_D (Π) for (POPC without and with PazePC/PoxnoPC)/SM/Chol (1.5/1.5/1 molar ratio) mixtures at 24 °C. OxPL-free system is represented by (■). Amount of PazePC was set as 12.5% (△) and 25% (●) of the phospholipid fraction. Data for PoxnoPC (25% of the PL fraction) is provided for comparison (◊). Corresponding Boltzmann fits are included. Dotted line indicates the data fit for pure POPC film.

the system reaches upper limit for diffusion times) is subsequently shorter in terms of time in comparison to the oxPL-free films.

5. Discussion

In the present study we assessed the impact of oxidatively truncated PCs on the integrity and dynamics of lipid "rafts" in monolayers. We could confirm that both studied oxidized PCs promote the stabilization of (SM/Chol) domains, presumably in the liquid ordered (L_o) phase. Upon comparing the two oxPLs, the aldehyde derivative seems to be more efficient in stabilizing the phase separation. As suggested by Khandelia & Mouritsen, the azelaoyl chain in PazePC would loop out from the hydrophobic core, with its preferential angle of orientation being 160 degrees with respect to the membrane normal [29]. On the other hand, the oxo-nonaoyl chain of PoxnoPC shows an angle distribution of approximately 80°, perpendicular to the membrane normal. Since choline in sphingomyelin is supposed to be oriented towards the membrane, there could be a hypothetical interaction between the oxygen in the truncated acyl chains of oxPLs and the nitrogen of choline moiety of sphingomyelin [30]. The difference in the orientation of the oxidatively truncated acyl chains of oxPLs could result in enhanced interaction of PoxnoPC and sphingomyelin and thus augmented stabilization of lipid domain structures as indicated in our experiments. The role of the negative partial charge of the carboxylic acid (COO^-) moiety in PazePC could also be significant. Indeed, possible association of the sodium counterions from the subphase should be more prominent with the fully reversed *sn*-2 acyl chains, making any interactions in the domain boundaries less probable.

Along with the possible interactions at the domain boundary, thickness mismatch has been widely accepted as an explanation for domain separation and stabilization. Support has been found from the lack of differences in average dipole density, along with the mismatch-induced line tension between separate phases [6]. Considering that the average angular orientations of the oxidized oxPC acyl chains are directed away from the hydrocarbon–air interface, the structural order in the L_d-phase chain region could be compromised at higher surface pressures. This would indeed induce larger thickness mismatch between L_o- and L_d-phases, when oxPCs are present. Anyhow, it is unclear whether the seemingly better domain stabilization by PoxnoPC compared to PazePC is due to increased height mismatch or possible tighter interactions with other membrane constituents, as discussed above.

Exponentially increasing diffusion times upon approaching the miscibility transition suggests that this transition is a continuous nonlinear event. Condensation effect would finally lead to the lack of sufficient thickness mismatch between the phases and eventually result in domain disintegration. Judged from a series of images obtained by WFM near the phase transition, we observed insignificant fraction of merging domains, suggesting that phase mixing is not due to domain merging. Instead, domains seem to merge randomly even in the low lateral pressure regime, whenever coming sufficiently close. According to Akimov et al., this would mean separation distances of only 1–2 nm [7]. In addition, the segmentation analysis performed for WFM images upon monolayer compression showed mean domain size distributions of (2.12 ± 0.61) μm, (1.91 ± 0.39) μm and (2.05 ± 0.48) μm for a system without oxPCs and for monolayers containing PazePC and PoxnoPC, respectively. Thus, we found no significant differences in domain sizes for different L_d-phase compositions, which is in contradiction with the notion that increasing line tension should promote larger domains [8].

6. Conclusions

In this work, we describe and quantify the effect of oxidatively truncated PCs on lipid diffusion in ternary lipid films. First, we show that the presence of PazePC in a POPC monolayer increases a lipid area by about 4 $Å^2$ in comparison to POPC monolayer. Second, we studied ternary "raft mixtures" and the impact of two oxPLs (PazePC and PoxnoPC) on L_o structures. Visualization of compression and expansion processes using WFM did show no significant differences in the domain morphology for oxPC-free and PazePC containing monolayers. However, lipid films with PoxnoPC exhibited numerous inhomogeneities upon a compression–expansion cycle. The surface pressure needed for the L_d–L_o miscibility transition increased in the sequence oxPC-free–PazePC–PoxnoPC. Fluorescence correlation spectroscopy allowed for quantification of miscibility transition pressures (11.7 mN/m for films with no oxPC, 18.7 mN/m for 9.4 mol% PazePC, and 20.4 mN/m for 9.4 mol% PoxnoPC containing lipid films). In conclusion, oxPCs prevent the disintegration of the lipid domains as confirmed by WFM and quantified using FCS, as previously demonstrated by Brewster-angle microscopy [6].

Acknowledgments

This research was supported by the Grant Agency of the Czech Republic (P106/12/G016). M.H. acknowledges financial support by AS CR via Praemium Academiae award. P.P. acknowledges travel grant from European Science Foundation (EuroMEMBRANE).

References

[1] P.K.J. Kinnunen, K. Kaarniranta, A.K. Mahalka, Protein-oxidized phospholipid interactions in cellular signaling for cell death: from biophysics to clinical correlations, Biochim. Biophys. Acta Biomembr. 1818 (2012) 2446–2455.

[2] R. Volinsky, P.K.J. Kinnunen, Oxidized phosphatidylcholines in membrane-level cellular signaling: from biophysics to physiology and molecular pathology, FEBS J. 280 (2013) 2806–2816.

[3] R. Volinsky, L. Cwiklik, P. Jurkiewicz, M. Hof, P. Jungwirth, P.K.J. Kinnunen, Oxidized phosphatidylcholines facilitate phospholipid flip-flop in liposomes, Biophys. J. 101 (2011) 1376–1384.

[4] V.A. Fadok, D.L. Bratton, S.C. Frasch, M.L. Warner, P.M. Henson, The role of phosphatidylserine in recognition of apoptotic cells by phagocytes, Cell Death Differ. 5 (1998) 551–562.

[5] S.J. Martin, C.P.M. Reutelingsperger, A.J. Mcgahon, J.A. Rader, R.C.A.A. Vanschie, D.M. Laface, D.R. Green, Early redistribution of plasma-membrane phosphatidylserine is a general feature of apoptosis regardless of the initiating stimulus—inhibition by overexpression of Bcl-2 and Abl, J. Exp. Med. 182 (1995) 1545–1556.

[6] R. Volinsky, R. Paananen, P.K.J. Kinnunen, Oxidized phosphatidylcholines promote phase separation of cholesterol-sphingomyelin domains, Biophys. J. 103 (2012) 247–254.

[7] S.A. Akimov, P.I. Kuzmin, J. Zimmerberg, F.S. Cohen, Y.A. Chizmadzhev, An elastic theory for line tension at a boundary separating two lipid monolayer regions of different thickness, J. Electroanal. Chem. 564 (2004) 13–18.

[8] D.W. Lee, Y.J. Min, P. Dhar, A. Ramachandran, J.N. Israelachvili, J.A. Zasadzinski, Relating domain size distribution to line tension and molecular dipole density in model cytoplasmic myelin lipid monolayers, Proc. Natl. Acad. Sci. U. S. A. 108 (2011) 9425–9430.

[9] J.P. Mattila, K. Sabatini, P.K.J. Kinnunen, Interaction of cytochrome c with 1-palmitoyl-2-azelaoyl-sn-glycero-3-phosphocholine: evidence for acyl chain reversal, Langmuir 24 (2008) 4157–4160.

[10] M. Gudmand, M. Fidorra, T. Bjornholm, T. Heimburg, Diffusion and partitioning of fluorescent lipid probes in phospholipid monolayers, Biophys. J. 96 (2009) 4598–4609.

[11] A. Filippov, G. Oradd, G. Lindblom, Lipid lateral diffusion in ordered and disordered phases in raft mixtures, Biophys. J. 86 (2004) 891–896.

[12] M.J. Saxton, K. Jacobson, Single-particle tracking: applications to membrane dynamics, Annu. Rev. Biophys. Biomol. 26 (1997) 373–399.

[13] B.L. Sprague, J.G. McNally, FRAP analysis of binding: proper and fitting, Trends Cell Biol. 15 (2005) 84–91.

[14] Y. Chen, B.C. Lagerholm, B. Yang, K. Jacobson, Methods to measure the lateral diffusion of membrane lipids and proteins, Methods 39 (2006) 147–153.

[15] R. Machan, M. Hof, Lipid diffusion in planar membranes investigated by fluorescence correlation spectroscopy, Biochim. Biophys. Acta Biomembr. 1798 (2010) 1377–1391.

[16] J. Widengren, U. Mets, R. Rigler, Fluorescence correlation spectroscopy of triplet-states in solution—a theoretical and experimental-study, J. Phys. Chem. 99 (1995) 13368–13379.

[17] P.F.F. Almeida, W.L.C. Vaz, T.E. Thompson, Lateral diffusion in the liquid-phases of dimyristoylphosphatidylcholine cholesterol lipid bilayers—a free-volume analysis, Biochemistry 31 (1992) 6739–6747.

[18] K. Tanaka, P.A. Manning, V.K. Lau, H. Yu, Lipid lateral diffusion in dilauroylphosphatidylcholine/cholesterol mixed monolayers at the air/water interface, Langmuir 15 (1999) 600–606.

[19] W.L.C. Vaz, R.M. Clegg, D. Hallmann, Translational diffusion of lipids in liquid-crystalline phase phosphatidylcholine multibilayers—a comparison of experiment with theory, Biochemistry 24 (1985) 781–786.

[20] P.F.F. Almeida, W.L.C. Vaz, T.E. Thompson, Lipid diffusion, free area, and molecular dynamics simulations, Biophys. J. 88 (2005) 4434–4438.

[21] E. Falck, M. Patra, M. Karttunen, M.T. Hyvonen, I. Vattulainen, Lessons of slicing membranes: Interplay of packing, free area, and lateral diffusion in phospholipid/cholesterol bilayers, Biophys. J. 87 (2004) 1076–1091.

[22] W.E. Momsen, J.M. Smaby, H.L. Brockman, The suitability of Nichrome for measurement of gas–liquid interfacial-tension by the Wilhelmy method, J. Colloid Interface Sci. 135 (1990) 547–552.

[23] A. Benda, M. Benes, V. Marecek, A. Lhotsky, W.T. Hermens, M. Hof, How to determine diffusion coefficients in planar phospholipid systems by confocal fluorescence correlation spectroscopy, Langmuir 19 (2003) 4120–4126.

[24] L. Beranova, L. Cwiklik, P. Jurkiewicz, M. Hof, P. Jungwirth, Oxidation changes physical properties of phospholipid bilayers: fluorescence spectroscopy and molecular simulations, Langmuir 26 (2010) 6140–6144.

[25] M. Stefl, R. Sachl, M. Amaro Olzynska, D. Savchenko, A. Deyneka, A. Hermetter, L. Cwiklika, J. Humpolickova, H. Hof, Comprehensive portrait of cholesterol containing oxidized membrane, Biochim. Biophys. Acta Biomembr. 1838 (2014) 1769–1776.

[26] R.F. Jacob, R.P. Mason, Lipid peroxidation induces cholesterol domain formation in model membranes, J. Biol. Chem. 280 (2005) 39380–39387.

[27] C.C. Lai, S.H. Yang, B.J. Finlaysonpitts, Interactions of monolayers of unsaturated phosphocholines with ozone at the air–water-interface, Langmuir 10 (1994) 4637–4644.

[28] J.F.D. Liljeblad, V. Bulone, E. Tyrode, M.W. Rutland, C.M. Johnson, Phospholipid monolayers probed by vibrational sum frequency spectroscopy: instability of unsaturated phospholipids, Biophys. J. 98 (2010) L50–L52.

[29] H. Khandelia, O.G. Mouritsen, Lipid gymnastics: evidence of complete acyl chain reversal in oxidized phospholipids from molecular simulations, Biophys. J. 96 (2009) 2734–2743.

[30] J. Aittoniemi, P.S. Niemela, M.T. Hyvonen, M. Karttunen, I. Vattulainen, Insight into the putative specific interactions between cholesterol, sphingomyelin, and palmitoyl-oleoyl phosphatidylcholine, Biophys. J. 92 (2007) 1125–1137.